SINGULARITY TRACES OF SINGLE DEGREE-OF-FREEDOM PLANAR LINKAGES THAT INCLUDE PRISMATIC AND REVOLUTE JOINTS

Saleh M. Almestiri *, **Andrew P. Murray***, **David H. Myszka***, **Charles W. Wampler**†

*Department of Mechanical and Aerospace Engineering

University of Dayton

Dayton, OH 45469

† General Motors R&D Center

Warren, Michigan 48090

*Email: almestiris2@udayton.edu

ABSTRACT

This paper presents a general method to construct a singularity trace for single degree-of-freedom, closed-loop linkages that include prismatic, in addition to, revolute joints. The singularity trace has been introduced in the literature as a plot that reveals the gross motion characteristics of a linkage relative to a designated input joint and design parameter. Previously, singularity traces were restricted to mechanisms composed of only rigid bodies and revolute joints. The motion characteristics identified on the plot include changes in the number of solutions to the forward kinematic position analysis (geometric inversions), singularities, and changes in the number of branches. To illustrate the adaptation of the general method to include prismatic joints, basic slider-crank and inverted slider-crank linkages are explored. Singularity traces are then constructed for more complex Assur IV/3 linkages containing multiple prismatic joints. These Assur linkages are of interest as they form an architecture that is commonly used for mechanisms capable of approximating a shape change defined by a general set of closed

curves.

1 Introduction

A *singularity trace* has been introduced as a tool to classify the general motion characteristics of a single-degree of freedom (DOF) linkage containing revolute joints [1]. For a designated input angle and design parameter, the general motion characteristics include the singularities, circuits and critical points, which are described below. Li et al. [2] generated the singularity trace for complex linkages, such as Stephenson and double-butterfly linkages.

Forward (direct) kinematic position analysis of a single DOF linkage involves determining all possible joint positions at a certain position of the input link [3]. The set of position equations defines a *motion curve*, which exhibits the relationship between the joint variables. For a given position of the input link, multiple positions of the other joints are expected since the governing loop equations are non-linear. Erdman et. al. [4] refers to each solution of the forward kinematic analysis as a *geometric inversion* (GI). The conventional method for solving the forward kinematic problem uses tangent-half-angle substitution for the output variables [5]. Porta et. al. [6] used relaxation techniques for position analysis of multiloop mechanisms. Alternatively, Wampler [7] presents the use of isotropic coordinates to formulate a set polynomial equations which determine the locations of the links.

The study of parallel mechanisms called attention to the importance of determining singular configurations during the design phase, and avoiding them while operating the mechanism [8]. Gosselin and Angeles [9] and Park and Kim [10] defined kinematic singularities as configurations in which the degrees of freedom of a linkage changes instantaneously. At singularity configurations, the instantaneous kinematics become undetermined [11, 12]. Gosselin and Angeles [9] classify singularities into three types, based on the instantaneous input-output relationship. The first type of singularity occurs when the output link is at a dead point. The second type occurs when the input link is at a dead point, and the third type requires a certain condition on the parameters of the linkage that leads to a moving output when the input is locked or no motion of the output when the input is moving. The presented work uses singluarity traces to determine the motion characterisitcs associated with a proposed single-degree-of-freedom linkage design. Accordingly, the second-type singularities (those related to the motion of the actuated joint) are of interest during solution rectification [13]. These input-related singularities are referred to as dead center positions, where the input link is no longer able to move the linkage and the mechanical advantage of the mechanism goes to zero [14]. These singularities appear on the motion curve as turning points with respect to the input link displacement. Chase and Mirth [15] defined the *circuit* of a linkage as the set of all assembly configurations achievable without disconnecting any of the joints. The region on a circuit between two singularities is defined as a branch.

When a physical parameter of a linkage becomes a variable, the singularities form a curve whose projection is called the singularity trace. The turning points on the singularity curve with respect to the design parameter are called *critical points*, where many correspond to the transition linkages as described by Murray et. al. [16].

Linkages, where one or more physical parameter is considered a variable, have been addressed in the literature. Larochelle et. al. [17,18] refer to them as reconfigurable planar motion generators. Toa [19] calls them adjustable mechanisms and Kota et. al. [20] describe them as adjustable robotic mechanisms or programmable mechanisms.

Determining linkage positions, singularities, and critical points requires solving polynomial systems. Solutions for such systems are possible through numerical algebraic geometry, which involves the application of numerical methods to determine all solutions of polynomial systems, generally over $\mathbb{C}$. Homotopy continuation is a numerical algebraic geometry technique that is able to determine all isolated solutions of a polynomial system [21]. Another approach for solving kinematic polynomial systems is interval analysis [22], also known as a subdivision technique [23]. A procedure is used to evaluate a set of conditions within interval analysis bounds, such as the existence of a workspace singularity [24,25]. Unlike homotopy, interval analysis uses local information related to the initial bounds to locate the real roots of the system. Interval analysis is ideally suited for systems with more real roots than complex roots [26].

This paper extends the general methodology to generate motion curves and singularity traces for single DOF mechanisms that include prismatic joints as well as revolute joints. The remainder of the paper is organized as follows. Section 2 presents the general methodology incorporating prismatic joints. Examples of the method are given in Section 3 with an offset slider-crank that has a fixed line of slide, and Section 4 with an inverted slider-crank having a moving line of slide. The method is applied to a three-loop, Assur IV/3 mechanism that is a common architecture used in rigid-body shape change.

2 GENERAL METHOD

This section presents the general method used to create singularity traces. Isotropic coordinates are used to represent the links as vectors in the complex plane, which are well suited for homotopy continuation. Loop closure equations are generated for a single DOF mechanism that includes revolute and prismatic joints. Subsequent methods are used to identify the singularities and determine the critical points of the linkage.

2.1 Loop Closure

Isotropic coordinates can be used to represent the vectors that form a linkage that includes only rotational joints [1]. A unit vector in the complex plane defined by θ_j can be represented in polar form by the variable and its conjugate as

$$\mathbf{T}_j = e^{i\theta_j}, \qquad \text{and} \qquad \overline{\mathbf{T}}_j = e^{-i\theta_j}, \tag{1}$$

which are called isotropic coordinates [7]. By substituting the Euler equivalents into Eq. (1), $\mathbf{T}_j = \cos\theta_j + i\sin\theta_j$ and $\overline{\mathbf{T}}_j = \cos\theta_j - i\sin\theta_j$. When constructing loop closure equations, the two variables $\mathbf{T}_j$ and $\overline{\mathbf{T}}_j$ can be considered as independent variables under the condition that $\mathbf{T}_j\overline{\mathbf{T}}_j = 1$. When rotated in the plane by angle θ_j, a rigid link of length a_j has isotropic coordinates $(a_j\mathbf{T}_j, a_j\overline{\mathbf{T}}_j)$.

If the mechanism includes a prismatic joint j, a_j is a joint variable while $\mathbf{T}_j$ is a function of $\mathbf{T}_k$, where k denotes the link that defines the line of slide. As outlined by Wampler [7], new variables $\mathbf{S}_j = a_j\mathbf{T}_k$ and $\overline{\mathbf{S}}_j = a_j\overline{\mathbf{T}}_k$ are defined to represent a prismatic joint.

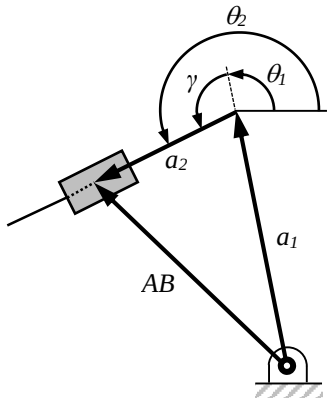

Fig. 1. Prismatic joint on a moving line of slide.

To illustrate with an example, Fig. 1 shows a portion of a mechanism where link 2 (the block) translates along a moving line of slide defined by θ_2. As the block moves, the joint variable a_2 changes. The angle γ is a link parameter, which is fixed. The angle of the moving line of slide is related to the revolute joint variable θ_1,

$$\theta_2 = \theta_1 + \gamma. \tag{2}$$

The vector **AB** can be written as

$$\mathbf{AB} = a_1\mathbf{T}_1 + a_2\mathbf{T}_2. \tag{3}$$

Substituting Eq. (2) into Eq. (1), $\mathbf{T}_2 = \mathbf{T}_1\mathbf{T}_\gamma$. Further substitution into Eq. (3) yields

$$\mathbf{AB} = a_1\mathbf{T}_1 + a_2\mathbf{T}_1\mathbf{T}_\gamma. \tag{4}$$

Defining $\mathbf{S}_2 = a_2\mathbf{T}_1$ and $\overline{\mathbf{S}}_2 = a_2\overline{\mathbf{T}}_1$, then

$$\mathbf{AB} = a_1\mathbf{T}_1 + \mathbf{S}_2\mathbf{T}_\gamma, \tag{5}$$

and the complex conjugate,

$$\overline{\mathbf{AB}} = a_1\overline{\mathbf{T}}_1 + \overline{\mathbf{S}}_2\overline{\mathbf{T}}_\gamma. \tag{6}$$

An identity equation can be written as $0 = \overline{\mathbf{T}}_1 a_2\mathbf{T}_1 - \mathbf{T}_1 a_2\overline{\mathbf{T}}_1 = \overline{\mathbf{T}}_1\mathbf{S}_2 - \mathbf{T}_1\overline{\mathbf{S}}_2$.

In summary, a prismatic joint j is incorporated into the general method by introducing $\mathbf{S}_j$ and $\overline{\mathbf{S}}_j$ into the loop closure equations to represent the variable a_j. An identity equation is also appropriately formulated. The method to determine singularities and critical points remains unchanged from Ref. [1], and is reviewed in the following sections for completeness.

2.2 Forward Kinematics

In the general analysis methodology, the linkage input variable is designated as $x \in \mathbb{C}$ and the design variable is $p \in \mathbb{C}$. All the remaining passive joint variables are $y \in \mathbb{C}^N$. Loop closure equations are formulated as

$$f(p,x,y) = 0, \qquad f : \mathbb{C}\times\mathbb{C}\times\mathbb{C}^N \to \mathbb{C}^N. \tag{7}$$

Considering a linkage that includes both m revolute and $n-m$ prismatic joints, the ℓ loop equations of Eq. (7) convert to $2\ell + n - 1$ equations in isotropic coordinates as:

$$\begin{aligned}
&\sum_{j=1}^{m} a_j\mathbf{T}_j + \sum_{k=m+1}^{n} \mathbf{S}_k\mathbf{T}_{\gamma_k} = 0,\\
&\sum_{j=1}^{m} \overline{a}_j\overline{\mathbf{T}}_j + \sum_{k=m+1}^{n} \overline{\mathbf{S}}_k\overline{\mathbf{T}}_{\gamma_k} = 0,\\
&\mathbf{T}_j\overline{\mathbf{T}}_j = \left(e^{i\theta_j}\right)\left(e^{-i\theta_j}\right) = 1, \qquad j = 2,\ldots,m,\\
&\overline{\mathbf{T}}_{k-1}\mathbf{S}_k - \mathbf{T}_{k-1}\overline{\mathbf{S}}_k = 0, \qquad k = m+1,\ldots,n.
\end{aligned} \tag{8}$$

In its most general form, the coefficients $a_j \in \mathbb{C}$ in Eq. (8) correspond to the line segments that connect the joints. The complex conjugates of the link edges $\overline{a}_j$ also appear. For a binary link, the vector $\mathbf{T}_j$ lies along the line that connects the

joints, in which case a_j is real, and $a_j = \overline{a}_j$. This is done throughout the examples in this paper. Also, note that $\mathbf{T}_j\overline{\mathbf{T}}_j = 1$, where j corresponds to any ground link, is not included as its angle θ_j is known. The system in Eq. (8) consists of $N+1$ equations in $N+2$ unknowns and for a given value of x produces a set of y values that correspond to geometric inversions of the linkage. Methods for solving the system of equations are discussed in [27]. The solutions in this paper were produced using numerical polynomial continuation homotopy methods implemented in using the Bertini software package [28].

2.3 Singularity Analysis

Finding all branches of the motion with respect to x is desirable. The branches on the motion curve meet at a singularity point. The singularity is a mechanism configuration where the driving link is unable to move the mechanism. For a fixed design parameter p, the tangent $[\Delta x, \Delta y]$ to the motion curve is given by

$$f_x \Delta x + f_y \Delta y = 0, \tag{9}$$

where $f_x = \frac{\partial f}{\partial x} \in \mathbb{C}^{N\times 1}$ and $f_y = \frac{\partial f}{\partial y} \in \mathbb{C}^{N\times N}$. The singularities occur when $\Delta y \neq 0$ with $\Delta x = 0$, which implies that

$$D(p,x,y) := \det f_y = 0. \tag{10}$$

Combining the loop closure and singularity conditions,

$$F(p,x,y) = \begin{bmatrix} f(p,x,y) \\ \\ D(p,x,y) \end{bmatrix}. \tag{11}$$

This system of $N+1$ equations in $N+1$ unknowns is solved to find the singularities.

2.4 Critical Points

To this point in the analysis, the design parameter p is considered fixed. As the design parameter is altered, the gross motion behavior of the linkage changes at critical points. The singularity curve consists of the singularities as p changes. The projection of the singularity curve into the plane of the input joint x and the design parameter p is known as the singularity trace. At certain values of p (termed critical points) the number of singularities change. The process of determining the critical points is analogous to the singularity problem, but replacing x by p, y by (x,y), and f by F. The tangency condition from Eq. (9) becomes

$$\frac{\partial F}{\partial p}\Delta p + \frac{\partial F}{\partial x}\Delta x + \frac{\partial F}{\partial y}\Delta y = 0. \tag{12}$$

Defining

$$F_{xy} = \begin{bmatrix} \frac{\partial F}{\partial x} \frac{\partial F}{\partial y} \end{bmatrix} = \begin{bmatrix} \frac{\partial f}{\partial x} \frac{\partial f}{\partial y} \\ \frac{\partial D}{\partial x} \frac{\partial D}{\partial y} \end{bmatrix}. \tag{13}$$

Critical points occur when $\Delta(x,y) \neq 0$ with $\Delta p = 0$, which implies

$$E := \det F_{xy} = 0. \tag{14}$$

Combining loop closure, singularity and critical point conditions generates a system of $N+2$ equations

$$\begin{bmatrix} f(p,x,y) \\ D(p,x,y) \\ E(p,x,y) \end{bmatrix} = 0 \tag{15}$$

in $N+2$ unknowns that include p, x, y. As before, the system is solved using Bertini and produces all critical points.

3 OFFSET SLIDER-CRANK LINKAGE

An offset slider-crank linkage is shown in Fig. 2 and provides a basic example of generating the singularity trace and motion curves. The linkage consists of four links, three revolute joints, and one prismatic joint on a fixed line of slide. The linkage input variable is designated as $x = \theta_1$. The other joint variables are $y = \{\theta_2, a_3\}$, and the design parameter is $p = a_1$. The physical parameters include a_2, θ_3, a_4, and θ_4. The line of slide and offset are orthogonal, making $\gamma = \theta_3 - \theta_4 = \pi/2$

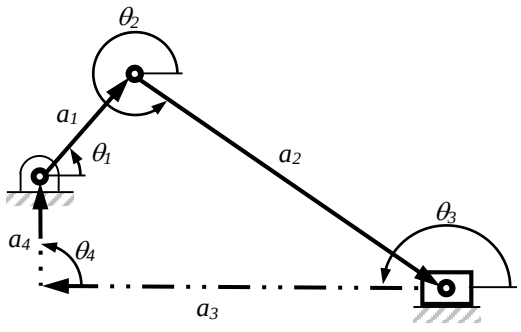

Fig. 2. The position vector loop for an offset, slider-crank linkage.

3.1 Loop Closure

As described in the previous section, a variable $\mathbf{S}_3 = a_3\mathbf{T}_4$ is defined to facilitate analysis of a linkage that include a prismatic joint. Note that in this example, $\mathbf{T}_4$ is a fixed value as the line of slide is fixed. Examples with a moving line of slide are provided in later sections. The loop closure equations are

$$\begin{aligned} g &:= a_1\mathbf{T}_1 + a_2\mathbf{T}_2 + \mathbf{S}_3\mathbf{T}_\gamma + a_4\mathbf{T}_4 = 0, \\ \overline{g} &:= a_1\overline{\mathbf{T}}_1 + a_2\overline{\mathbf{T}}_2 + \overline{\mathbf{S}}_3\overline{\mathbf{T}}_\gamma + a_4\overline{\mathbf{T}}_4 = 0, \\ h_j &:= \mathbf{T}_j\overline{\mathbf{T}}_j - 1 = 0, \quad j = 1,2, \\ q_3 &:= \overline{\mathbf{T}}_4\mathbf{S}_3 - \mathbf{T}_4\overline{\mathbf{S}}_3 = 0. \end{aligned} \tag{16}$$

Since θ_3 and θ_4 are fixed with the frame, h_3 and h_4 are not required.

3.2 Forward Kinematics

The system in Eq. (16) is rewritten to eliminate $\mathbf{T}_2$ and $\overline{\mathbf{T}}_2$,

$$\begin{aligned} R_2 &:= -a_2\mathbf{T}_2 = a_1\mathbf{T}_1 + \mathbf{S}_3\mathbf{T}_\gamma + a_4\mathbf{T}_4, \\ \overline{R}_2 &:= -a_2\overline{\mathbf{T}}_2 = a_1\overline{\mathbf{T}}_1 + \overline{\mathbf{S}}_3\overline{\mathbf{T}}_\gamma + a_4\overline{\mathbf{T}}_4. \end{aligned} \tag{17}$$

Since $a_2 \neq 0$, $a_2^2 h_2 = 0$, which leads to $R_2\overline{R}_2 - {a_2}^2 = 0$. Expanding,

$$H_2 := (a_1\mathbf{T}_1 + \mathbf{S}_3\mathbf{T}_\gamma + a_4\mathbf{T}_4)(a_1\overline{\mathbf{T}}_1 + \overline{\mathbf{S}}_3\overline{\mathbf{T}}_\gamma + a_4\overline{\mathbf{T}}_4) - a_2^2 = 0. \tag{18}$$

In this example, $\theta_4 = \gamma = \pi/2$, producing $\mathbf{T}_4 = \mathbf{T}_\gamma = i$ and $\overline{\mathbf{T}}_4 = \overline{\mathbf{T}}_\gamma = -i$.

When solving the forward kinematic problem, the design parameter is considered fixed. The designated input angle, θ_1 is selected making $\mathbf{T}_1$ known. Equation (18) and q_3 establish a system of two equations (one linear and one quadratic), which can be readily solved for $\{\mathbf{S}_3, \overline{\mathbf{S}}_3\}$. The joint variables are determined by using $a_3 = \sqrt{\overline{\mathbf{S}}_3\mathbf{S}_3}$ and $\mathbf{T}_2 = -R_2/a_2$. Each solution to the direct kinematic problem corresponds with a GI.

3.3 Singularity Points

To find singularity points, the input angle θ_1 becomes a variable and the design parameter remains fixed. Applying the singularity condition of Eq. (10) to the slider-crank gives

$$D := \det\left[\frac{\partial H_2}{\partial a_3}\right] = a_1(\overline{\mathbf{T}}_1\mathbf{T}_\gamma\mathbf{T}_4 + \mathbf{T}_1\overline{\mathbf{T}}_\gamma\overline{\mathbf{T}}_4) + a_4(\overline{\mathbf{T}}_\gamma + \mathbf{T}_\gamma) + 2\mathbf{S}_3\overline{\mathbf{T}}_4 = 0. \tag{19}$$

Equations (18), (19), h_1 and q_3 establish a system of four equations for $\{\mathbf{T}_1, \overline{\mathbf{T}}_1, \mathbf{S}_3, \overline{\mathbf{S}}_3\}$. Because the isotropic coordinates are treated as independent variables, actual solutions are those where $|\mathbf{T}_1| = \left|\overline{\mathbf{T}}_1\right| = 1$, and $\overline{\mathbf{S}}_3\mathbf{S}_3 \in \mathbb{R}$.

3.4 Critical Points

To determine the critical points, the design parameter a_1 is considered variable. Applying the singularity condition of Eq. (14) to the offset slider-crank,

$$E := \det \begin{bmatrix} \frac{\partial H_2}{\partial \theta_1} & \frac{\partial H_2}{\partial a_3} \\ \frac{\partial D}{\partial \theta_1} & \frac{\partial D}{\partial a_3} \end{bmatrix} = \mathbf{T}_1(\overline{\mathbf{T}}_\gamma \overline{\mathbf{S}}_3 + a_4 \overline{\mathbf{T}}_4) - \overline{\mathbf{T}}_1(\mathbf{T}_\gamma \mathbf{S}_3 - a_4 \mathbf{T}_4) = 0. \tag{20}$$

When solving for the critical points, Eqs. (18), (19), (20), h_1 and q_3 establish a system of five equations for $\{a_1, \mathbf{T}_1, \overline{\mathbf{T}}_1, \mathbf{S}_3, \overline{\mathbf{S}}_3\}$. As before, actual solutions are those where $|\mathbf{T}_1| = \left|\overline{\mathbf{T}}_1\right| = 1$, and $\overline{\mathbf{S}}_3\mathbf{S}_3 \in \mathbb{R}$.

3.5 Motion Curve and Singularity Trace

Using the critical points and singularity conditions, the methods presented in Ref. [1] were used to generate the singularity trace of the offset, slider-crank mechanism shown in Fig. 3. The physical parameters selected are $a_2 = 6.00$, $a_4 = 1.00$, $\theta_3 = \pi$, and $\theta_4 = \pi/2$. The singularity trace for the slider crank mechanism is observed to be an open ended singularity trace, meaning that GI's exist for any length of a_1. The critical points occur at $(\theta_1, a_1) = \{(1.57, 5.00), (-1.57, 7.00)\}$. As shown in Fig. 3, the plot contains *regions* bounded by the singularity curve and have the same number of GIs. Critical points represent values of the design parameter that are associated with a change in the number of singularities. Since each of these critical points occur on the singularity trace where the slope is zero, a change in the number of circuits is observed at the critical points (see [1]). Horizontal lines at values critical values of a_1 divide the singularity trace of Fig. 3 into three *zones* and have the same number of circuits. In the first zone is $0 < a_1 < 5$, two GI are possible for any value of θ_1. This represents two assembly circuits, where both segments of the motion curve run smoothly from $-\pi$ to π with no singularities. The second zone of the singularity trace is $5 < a_1 < 7$. Selecting $a_1 = 6.0$, the motion curve has one circuit and two singularities at $\theta_1 = 0.99$ and 2.16. Over the period when $-\pi < \theta_1 < 0.99$ and $2.15 < \theta_1 < \pi$, the linkages has 2 GIs. The linkage has 0 GIs for $0.99 < \theta_1 < 2.15$, which means the mechanism cannot be assembled. The third zone of the singularity trace is $a_1 > 7$. Selecting $a_1 = 8.50$ the motion curve has two circuits and four singularities at $\theta_1 = -2.17, -0.97, 0.63$, and 2.51. The linkage can only be assembled and has 2 GIs over $-\pi < \theta_1 < -2.17$, $-0.97 < \theta_1 < 0.63$, and $2.51 < \theta_1 < \pi$.

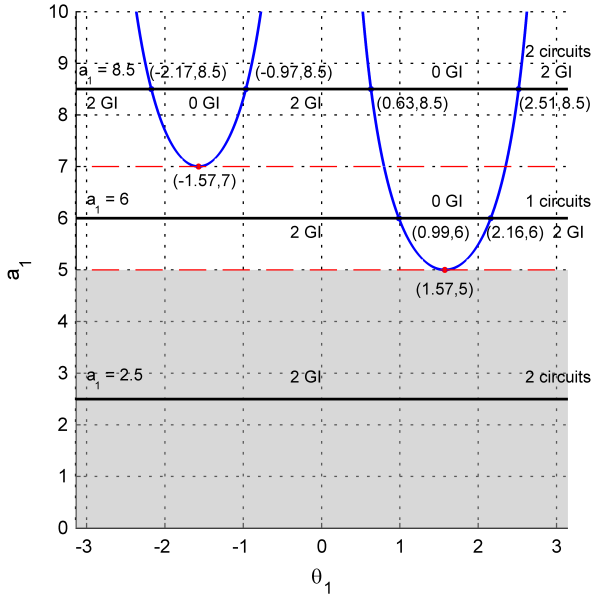

Fig. 3. The slider-crank singularity trace. Red markers represent the critical points. Regions of equal GI and circuits are identified. Singularities at different values of a_1 are indicated. Both circuits within the gray zone exhibit a fully rotatable crank.

3.6 Validation

Being a very common and basic mechanism, most machine theory texts manipulate the loop closure equations for the offset, slider-crank linkage to form a single equation [3,4]. One version relates a_3 and θ_1,

$$a_3^2 + Ba_3 + C = 0, \tag{21}$$

where $B = -2a_1\cos\theta_1$ and $C = a_1^2 + a_4^2 - a_2 + 2a_1a_4\sin\theta_1$. The motion curve resulting from Eq. (18) and Eq. (21) are identical. Further, Murray et al., [16] outline the transition conditions for the offset, slider-crank as being $a_1 = a_2 - a_1$ and $a_1 = a_2 + a_4$. Substituting $a_2 = 6.00$ and $a_4 = 1.00$ result in $a_1 = 5.00$ and 7.00, which correspond with the critical points identified in Fig. 3.

4 INVERTED SLIDER CRANK LINKAGE

An inverted slider-crank linkage is shown in Fig. 4. This linkage includes a prismatic joint that translates along a moving line of slide. The linkage input variable is designated as $x = \theta_1$, the other joint variables are $y = \{a_2, \theta_3\}$, and the design parameter is $p = a_1$. The physical parameters include a_3, γ, a_4, and θ_4.

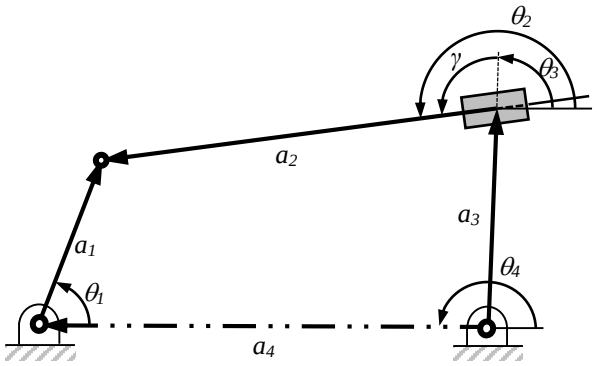

Fig. 4. Inverted slider-crank linkage position vector loop.

4.1 Loop Closure

The variable $\mathbf{S}_2 = a_2\mathbf{T}_3$ is defined to include the prismatic joint. The loop closure equations are

$$\begin{aligned} g &:= a_3\mathbf{T}_3 + \mathbf{T}_\gamma\mathbf{S}_2 - a_4\mathbf{T}_4 - a_1\mathbf{T}_1 = 0, \\ \overline{g} &:= a_3\overline{\mathbf{T}}_3 + \overline{\mathbf{T}}_\gamma\overline{\mathbf{S}}_2 - a_4\overline{\mathbf{T}}_4 - a_1\overline{\mathbf{T}}_1 = 0, \\ h_j &:= \mathbf{T}_j\overline{\mathbf{T}}_j - 1 = 0 \quad j = 1,3, \\ q_2 &:= \overline{\mathbf{T}}_3\mathbf{S}_2 - \mathbf{T}_3\overline{\mathbf{S}}_2 = 0. \end{aligned} \tag{22}$$

Since the frame is designated $j = 4$ and θ_2 depends on θ_3, then h_2 and h_4 are not required.

4.2 Forward Kinematics

Eliminating $\mathbf{S}_2$ and $\overline{\mathbf{S}}_2$ from Eq. (22),

$$\begin{aligned} R_2 &:= \mathbf{T}_\gamma\mathbf{S}_2 = a_1\mathbf{T}_1 + a_4\mathbf{T}_4 - a_3\mathbf{T}_3, \\ \overline{R}_2 &:= \overline{\mathbf{T}}_\gamma\overline{\mathbf{S}}_2 = a_1\overline{\mathbf{T}}_1 + a_4\overline{\mathbf{T}}_4 - a_3\overline{\mathbf{T}}_3. \end{aligned} \tag{23}$$

Using q_2 with the identity $\mathbf{T}_\gamma\overline{\mathbf{T}}_\gamma = 1$, $\overline{\mathbf{T}}_3\overline{\mathbf{T}}_\gamma R_2 - \mathbf{T}_3\mathbf{T}_\gamma\overline{R}_2 = 0$. Expanding,

$$H_2 := \overline{\mathbf{T}}_3\overline{\mathbf{T}}_\gamma(a_1\mathbf{T}_1 + a_4\mathbf{T}_4 - a_3\mathbf{T}_3) - \mathbf{T}_3\mathbf{T}_\gamma(a_1\overline{\mathbf{T}}_1 + a_4\overline{\mathbf{T}}_4 - a_3\overline{\mathbf{T}}_3) = 0. \tag{24}$$

When solving the forward kinematic problem, the design parameter is considered to be fixed. With designated input angle, θ_1 (ie., $\mathbf{T}_1$ known), Eq. (24) and h_3 establishes a system of two equations for $\{\mathbf{T}_3, \overline{\mathbf{T}}_3\}$. The prismatic joint variable is determined by using $a_2 = \sqrt{\mathbf{S}_2\overline{\mathbf{S}}_2}$. Each solution to the direct kinematic problem represents a GI.

4.3 Singularity Points

To determine the singularity points, the input angle θ_1 becomes a variable and the design parameter remains fixed. Applying the singularity condition of Eq. (10) to the inverted slider-crank gives

$$D := \det\left[\frac{\partial H_2}{\partial \theta_3}\right] = \overline{\mathbf{T}}_3\overline{\mathbf{T}}_\gamma(a_1\mathbf{T}_1 + a_4\mathbf{T}_4) + \mathbf{T}_3\mathbf{T}_\gamma(a_1\overline{\mathbf{T}}_1 + a_4\overline{\mathbf{T}}_4) = 0. \tag{25}$$

When solving for the singularity points, Eqs. (24), (25), h_1 and h_3 establish a system of four equations for $\{\mathbf{T}_1, \overline{\mathbf{T}}_1, \mathbf{T}_3, \overline{\mathbf{T}}_3\}$. Because the isotropic coordinates are treated as independent variables, actual solutions are those where $|\mathbf{T}_1| = \left|\overline{\mathbf{T}}_1\right| = |\mathbf{T}_3| = \left|\overline{\mathbf{T}}_3\right| = 1$.

4.4 Critical Points

To determine the critical points, the design parameter a_1 is considered a variable. Applying the critical point condition of Eq. (14) to the inverted slider-crank,

$$E := \det\begin{bmatrix} \frac{\partial H_2}{\partial \theta_1} & \frac{\partial H_2}{\partial \theta_3} \\ \frac{\partial D}{\partial \theta_1} & \frac{\partial D}{\partial \theta 3} \end{bmatrix} = \mathbf{T}_1\overline{\mathbf{T}}_4 - \overline{\mathbf{T}}_1\mathbf{T}_4 = 0. \tag{26}$$

When solving for the critical points, Eqs. (24), (25), (26), h_1 and h_3 establish a system of five equations for $\{a_1, \mathbf{T}_1, \overline{\mathbf{T}}_1, \mathbf{T}_3, \overline{\mathbf{T}}_3\}$. Actual solutions are those where $a_1 = \overline{a}_1$ and $|\mathbf{T}_1| = \left|\overline{\mathbf{T}}_1\right| = |\mathbf{T}_3| = \left|\overline{\mathbf{T}}_3\right| = 1$.

4.5 Motion Curve and Singularity Trace

Using physical parameter values of $a_3 = 0.6$, $a_4 = 1$, $\theta_4 = \pi$, $\gamma = 1.2$, the singularity trace of the inverted slider-crank mechanism is given in Fig. 5. Again, each of these critical points occur on the singularity trace where the slope is zero. Thus, a change in the number of circuits is observed each critical point: $(\theta_1, a_1) = \{(0, 0.44), (0, 1.56)\}$. Also observed is that for values of $a_1 < 0.44$ and $a_1 > 1.56$, the linkage has a fully rotating crank.

Regions in the singularity trace bounded by the singularity curve have the same number of GIs. The singularity trace is further divided into three zones based on the values of a_1 at the critical points. The first zone is $0 < a_1 < 0.44$, the second is $0.44 < a_1 < 1.56$, and the third zone $a_1 > 1.56$. By generating the motion curve for the mechanism at a certain values of a_1, the number of GIs and circuits are identified for each zone and region in the the singularity trace.

Figure 6 shows traces of the motion curve at $a_1 = 0.2$, 0.3, and 0.4, projected onto θ_1-θ_3 plane. For each value of a_1, two assembly circuits exist and 2 GIs are possible for any value of θ_1. For each circuit, the linkage has a fully rotating crank

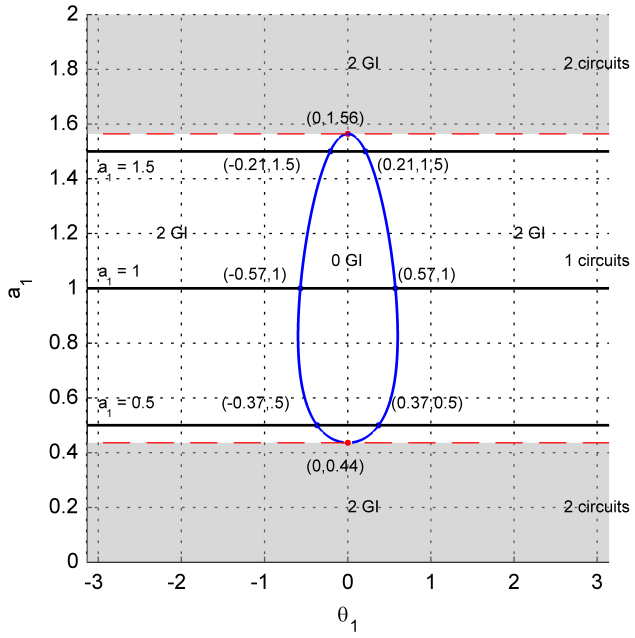

Fig. 5. The inverted slider-crank singularity trace. Red markers denote the critical points. Region of equal GIs and circuits are identified. Singularities at different values of a_1 are indicated. Both circuits within the gray zones exhibit a fully rotatable crank.

as all GI branches extend from $-\pi$ to π. This zone on the singularity trace has two GIs, two circuits, and no singularities. Thus, a first zone linkage contains two circuits that have an oscillating output with a fully rotational input.

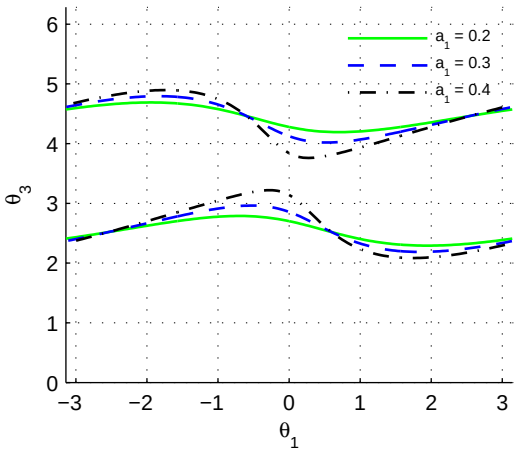

Fig. 6. Traces of the motion curve at various lengths of $a_1 = 0.2, 0.3$, and 0.4, from the first zone on the singularity trace.

In the second zone of the singularity trace, two singularities exist for a selected value of a_1. Figure 7 shows traces of the motion curve at $a_1 = 0.5$, 1.0, and 1.5, projected onto θ_1-θ_3. For each value of a_1, the motion curve has one assembly circuit and two singularity points denoted with red markers. Outside the red markers, the linkage has two GIs. In the region

between the red markers, the linkage has 0 GIs, which means the mechanism cannot be assembled. With a linkage in this second zone, two GIs are possible that only permit an oscillating input producing an oscillating output.

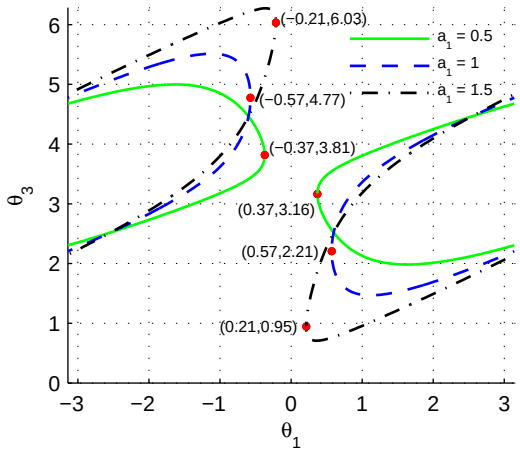

Fig. 7. Traces of the motion curve at various lengths of $a_1 = 0.5$, 1.0, and 1.5, from the second zone on the singularity trace. Singularity points are identified with red markers.

Figure 8 shows traces of the motion curve from the third zone of the singularity trace curve with $a_1 = 1.58$, 1.65,and 2.00. For all values of θ_1, the linkage has two GIs and two circuits with no singularities. A third zone linkage contains two circuits that have a fully rotating output with a fully rotational input.

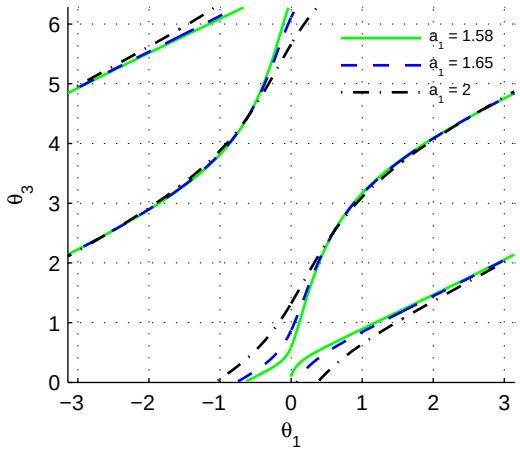

Fig. 8. Traces of the motion curve at various lengths of $a_1 = 1.58$, 1.65,and 2.00, from the third zone on the singularity trace.

4.6 Validation

The analysis of the inverted slider-crank linkage is included in most machine theory texts [3, 4]. A single equation relating θ_3 and θ_1 is stated as

$$D\sin(\theta_2) - E\cos(\theta_2) - a_3\sin(\gamma) = 0, \tag{27}$$

where $D = a_1\cos(\theta_1) - a_4\cos(\theta_4)$ and $E = a_1\sin(\theta_1) + a_4\sin(\theta_4)$. The resulting motion curves from Eq. (24) and Eq. (27) are identical. Additionally, Murray et al., [16] outline the transition conditions for the inverted, slider-crank as being $a_1 = a_4 + a_3\sin\gamma$ and $a_1 = a_4 + a_3\sin\gamma$. Substituting the values of physical parameters $a_3 = 0.6$, $a_4 = 1.0$, $\gamma = 1.2$ result in $a_1 = 0.44$ and 1.56, which correspond with the critical points identified in Fig. 5.

In the two examples previously discussed and those produced in Refs. [1, 2], a link length has been selected as a design parameter. It is noted that the fixed angle γ could be designated as a design parameter without changing the general method.

5 ASSUR IV/3 with TWO PRISMATIC JOINTS

The general motion analysis method is applied to the linkage shown in Fig. 9, which is classified an an Assur Class IV, Order 3, denoted Assur IV/3 [29]. This is an example of a kinematic architecture used in planar rigid-body mechanisms used to approximate shape changes defined by closed curves [30]. Links 11, 12, 13, and 14 constitute a closed loop connected by revolute and prismatic joints that has the capacity to vary between specific shapes in a controlled manner. Applications for such shape change mechanisms include morphing aircraft wings [31] and variable geometry dies for polymer extrusion [32].

The input variable is $x = \theta_1$, the design parameter is $p = a_1$, and the passive joint variables are $y = \{\theta_2, \theta_3, a_4, a_7, \theta_9, \theta_{14}\}$.

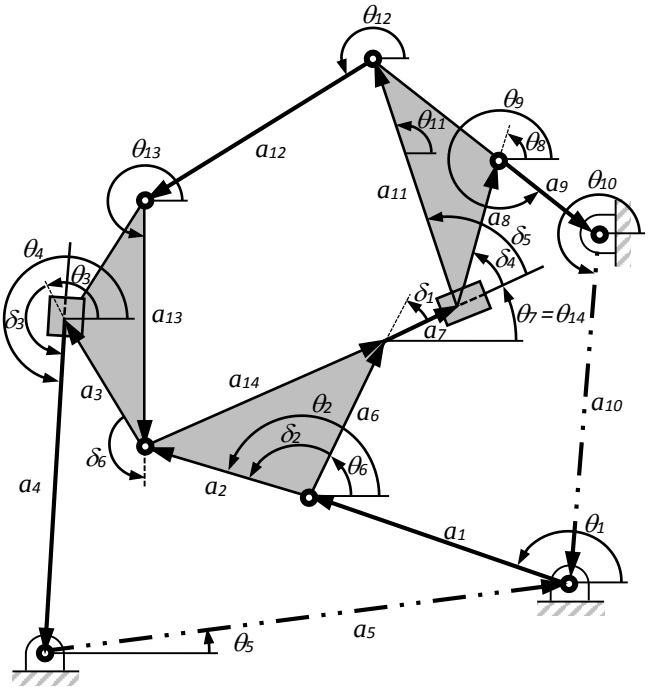

Fig. 9. Assur IV/3 linkage position vector loop.

5.1 Loop Closure

The variables $\mathbf{S}_4 = a_4\mathbf{T}_3$ and $\mathbf{S}_7 = a_7\mathbf{T}_{14}$ are defined to represent the prismatic joints that slide along links 4 and 7, respectively. The loop closure conditions and appropriate identities are

$$
\begin{aligned}
g_1 &:= a_1\mathbf{T}_1 + a_2\mathbf{T}_2 + a_3\mathbf{T}_3 + \mathbf{T}_{\delta_3}\mathbf{S}_4 + a_5\mathbf{T}_5 = 0,\\
g_2 &:= a_1\mathbf{T}_1 + a_6\mathbf{T}_6 + \mathbf{S}_7 + a_8\mathbf{T}_8 + a_9\mathbf{T}_9 + a_{10}\mathbf{T}_{10} = 0,\\
g_3 &:= a_{11}\mathbf{T}_{11} + a_{12}\mathbf{T}_{12} + a_{13}\mathbf{T}_{13} + a_{14}\mathbf{T}_{14} + \mathbf{S}_7 = 0,\\
h_j &:= \overline{\mathbf{T}}_j\mathbf{T}_j - 1 = 0 \quad j = 1,3,9,12,14,\\
q_4 &:= \mathbf{T}_3\overline{\mathbf{S}}_4 - \overline{\mathbf{T}}_3\mathbf{S}_4 = 0,\\
q_7 &:= \mathbf{T}_{14}\overline{\mathbf{S}}_7 - \overline{\mathbf{T}}_{14}\mathbf{S}_7 = 0.
\end{aligned}
\tag{28}
$$

5.2 Forward Kinematics

The fixed angular relationships on the ternary links are represented with $\mathbf{T}_2 = \mathbf{T}_{\delta_1}\mathbf{T}_{\delta_2}\mathbf{T}_{14}$, $\mathbf{T}_6 = \mathbf{T}_{\delta_1}\mathbf{T}_{14}$, $\mathbf{T}_8 = \mathbf{T}_{\delta_4}\mathbf{T}_{14}$, $\mathbf{T}_{11} = \mathbf{T}_{\delta_5}\mathbf{T}_{14}$, and $\mathbf{T}_{13} = \mathbf{T}_{\delta_6}\mathbf{T}_3$. Variables $\{\mathbf{S}_4, \overline{\mathbf{S}}_4, \mathbf{T}_9, \overline{\mathbf{T}}_9, \mathbf{T}_{12}, \overline{\mathbf{T}}_{12}\}$ can be eliminated by rewriting and manipulating

Eqs. (28),

$$
\begin{aligned}
R_4 &:= -\overline{\mathbf{T}}_3\mathbf{S}_4 = \overline{\mathbf{T}}_{\delta_3}\overline{\mathbf{T}}_3(a_1\mathbf{T}_1 + a_2\mathbf{T}_{\delta_1}\mathbf{T}_{\delta_2}\mathbf{T}_{14} + a_3\mathbf{T}_3 + a_5\mathbf{T}_5),\\
R_9 &:= -a_9\mathbf{T}_9 = a_1\mathbf{T}_1 + (a_6\mathbf{T}_{\delta_1} + a_8\mathbf{T}_{\delta_4})\mathbf{T}_{14} + \mathbf{S}_7 + a_{10}\mathbf{T}_{10},\\
R_{12} &:= -a_{12}\mathbf{T}_{12} = (a_{11}\mathbf{T}_{\delta_5} + a_{14})\mathbf{T}_{14} + a_{13}\mathbf{T}_{\delta_6}\mathbf{T}_3 + \mathbf{S}_7.
\end{aligned}
\tag{29}
$$

The conjugates $\overline{R}_4$, $\overline{R}_9$, and $\overline{R}_{12}$ are also formed. The identity equations h_9, h_{12}, and q_4 are used to achieve the reduced form of the loop closure, which can be expressed as follows

$$
\begin{aligned}
Q_4 &:= R_4 - \overline{R}_4 = 0,\\
H_9 &:= R_9\overline{R}_9 - a_9^2 = 0,\\
H_{12} &:= R_{12}\overline{R}_{12} - a_{12}^2 = 0.
\end{aligned}
\tag{30}
$$

For an input value of θ_1, Eqs. (30) coupled with h_3, h_{14}, and q_7 form a system of six equations in the variables $\{\mathbf{T}_3, \overline{\mathbf{T}}_3, \mathbf{T}_{14}, \overline{\mathbf{T}}_{14}, \mathbf{S}_7, \overline{\mathbf{S}}_7\}$. The solutions can be obtained from Bertini to determine the passive joint positions. As before, actual solutions are those where $|\mathbf{T}_3| = \left|\overline{\mathbf{T}}_3\right| = |\mathbf{T}_{14}| = \left|\overline{\mathbf{T}}_{14}\right| = 1$ and $\overline{\mathbf{S}}_7\mathbf{S}_7 \in \mathbb{R}$. The prismatic joint variable is determined by using $a_7 = \sqrt{\mathbf{S}_7\overline{\mathbf{S}}_7}$.

5.3 Singularity Points

The singularity points for the Assur IV/3 are obtained by solving the system of equations that includes Eqs. (30), h_1, h_3, h_{14}, and q_7 along with the singularity condition equation,

$$
D := \det\begin{bmatrix}
\frac{\partial H_4}{\partial\theta_3} & \frac{\partial H_4}{\partial\theta_{14}} & \frac{\partial H_4}{\partial a_7}\\
\frac{\partial H_9}{\partial\theta_3} & \frac{\partial H_9}{\partial\theta_{14}} & \frac{\partial H_9}{\partial a_7}\\
\frac{\partial H_{12}}{\partial\theta_3} & \frac{\partial H_{12}}{\partial\theta_{14}} & \frac{\partial H_{12}}{\partial a_7}
\end{bmatrix} = 0.
\tag{31}
$$

The solution to the system of seven equations with seven unknowns can be obtained from Bertini to determine the the input and passive joint positions that place the linkage in a singularity.

5.4 Critical Points

To find the critical points of the linkage, the design parameter is set to be a variable and one more equation is added to the system from the singularity analysis, so that the number of unknowns equals the number of equations. The additional

equation is given by

$$E := \det \begin{bmatrix} \frac{\partial H_4}{\partial \theta_1} & \frac{\partial H_4}{\partial \theta_3} & \frac{\partial H_4}{\partial \theta_{14}} & \frac{\partial H_4}{\partial a_7} \\ \frac{\partial H_9}{\partial \theta_1} & \frac{\partial H_9}{\partial \theta_3} & \frac{\partial H_9}{\partial \theta_{14}} & \frac{\partial H_9}{\partial a_7} \\ \frac{\partial H_{12}}{\partial \theta_1} & \frac{\partial H_{12}}{\partial \theta_3} & \frac{\partial H_{12}}{\partial \theta_{14}} & \frac{\partial H_{12}}{\partial a_7} \\ \frac{\partial D}{\partial \theta_1} & \frac{\partial D}{\partial \theta_3} & \frac{\partial D}{\partial \theta_{14}} & \frac{\partial D}{\partial a_7} \end{bmatrix} = 0. \tag{32}$$

The solution to the system of eight equations with eight unknowns can be obtained from Bertini to determine the the design parameter value, input and passive joint positions that place the linkage at a critical point.

5.5 Singularity Trace

For this numerical example, the physical parameters are set to $a_2 = 0.72$, $a_3 = 0.77$, $a_5 = 0.87$, $a_6 = 0.57$, $a_8 = 0.53$, $a_9 = 0.9$, $a_{10} = 1.546$, $a_{11} = 0.65$, $a_{12} = 1.34$, $a_{13} = 0.6$, $a_{14} = 1.09$, $\theta_5 = 0$, $\theta_{10} = -2.926$, $\delta_1 = 2.015$, $\delta_2 = 1.727$, $\delta_3 = 0.634$,$\delta_4 = 0.981$, $\delta_5 = 1.487$, and $\delta_6 = 0.356$. The singularity trace of the Assur IV/3 linkage with the design variable a_1 is shown in Figure 10. The singularity trace is divided into zones with the same number of circuits, and regions with with same number of GIs. As the design parameter varies, the number of circuits changes by one when the critical point occurs at a smooth extrema. Critical points that appear on the plot as a cusp correspond to a point where the linkage moves into a different region of GIs. By setting $a_1 = 0.22$, and allowing a_{12} to vary, a second singularity trace can be obtained with new critical points as shown in Fig. 11

5.6 Motion Curve

Figure 12 shows a motion curve with $a_1 = 0.25$ projected onto θ_1-θ_2 plane. At this driving link length, the linkage has six circuits, five of them have continuously rotating cranks. Additionally, the sixth circuit exhibits two singularity points, between which is a linkage that is able to rotate greater than one full revolution. That is, the linkage upon return to the same value of the input link angle is placed into a different GI without encountering a singularity. As observed in Ref. [1], this motion characteristic is associated with being near a cusp on the singularity trace.

6 CONCLUSIONS

This paper illustrated a general method for generating the critical points and the singularity trace for any planar single DOF, closed loop linkage with a design parameter. The linkage may consist of rigid bodies connected by revolute joints and prismatic joints, which could be translating along a fixed or moving line of slide. As part of the process, forward

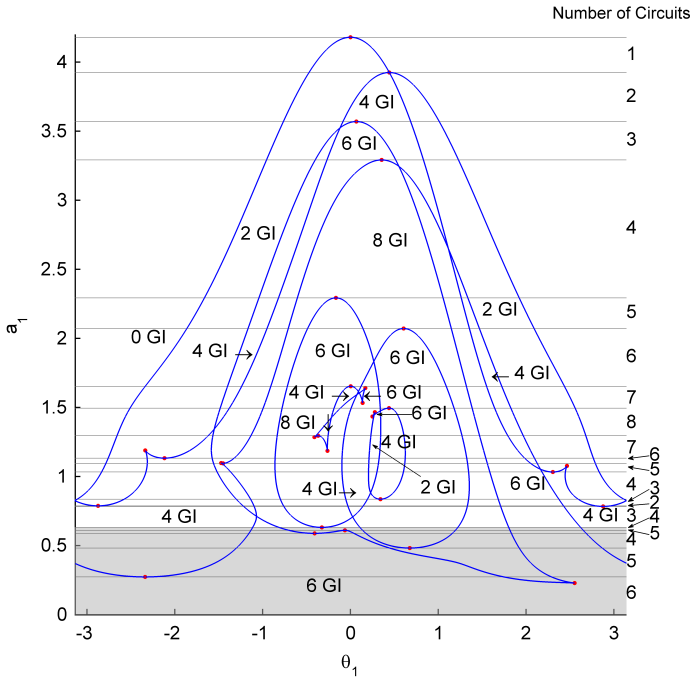

Fig. 10. The singularity trace for Assur IV/3 with respect to a_1. Red markers denote the critical points. Regions of equal GIs and circuits are identified. The zone shaded in gray contains at least one circuit with a fully rotatable crank.

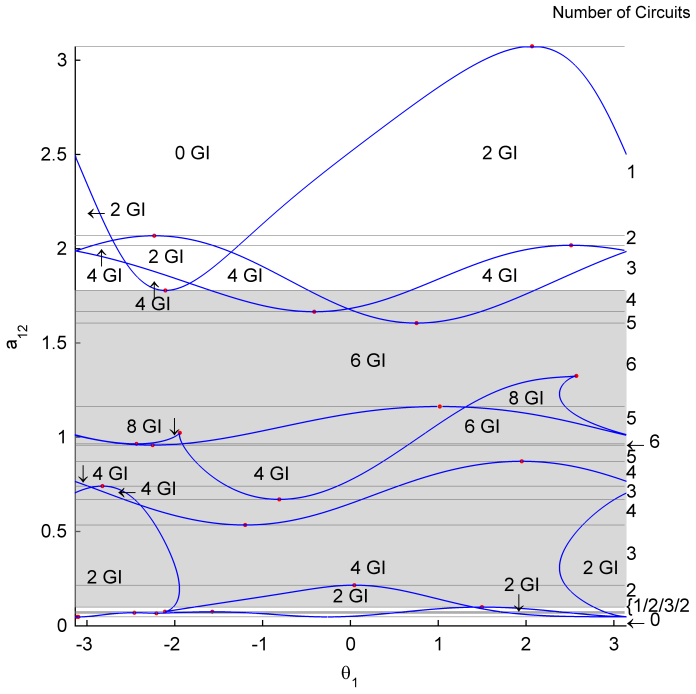

Fig. 11. The singularity trace for Assur IV/3 with respect to a_{12}. Red markers denote the critical points. The zone shaded in gray contains at least one circuit with a fully rotatable crank

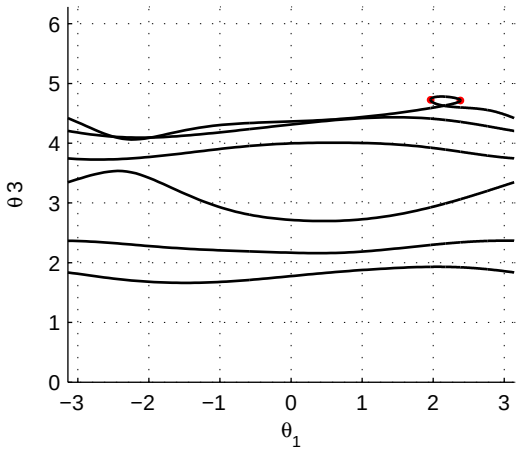

Fig. 12. Motion curve for Assur IV/3 with $a_1 = 0.25$ projected onto θ_1-θ_3.

kinematics, singularity points, and motion curves were developed. The method was applied to three different mechanisms with different levels of complexity to develop all facets of the use of the additional theory. The numerical examples show the formulation applied to a slider-crank, inverted slider crank, and an Assur IV/3 mechanism. Singularity traces for each linkage were generated and motion curves were plotted to fully understand the mechanism behavior on each zone and region of the singularity trace.

ACKNOWLEDGEMENT

This material is based upon work supported by the National Science Foundation under Grant No. #1234374. This work has been supported in part by the University of Dayton Office for Graduate Academic Affairs through the Graduate Student Summer Fellowship Program. The first author would like to express his sincere appreciation and deep gratitude to the Ministry of Higher Education of Libya and Misurata University for their financial support.

References

[1] Myszka, D. H., Murray, A. P., and Wampler, C. W., 2014. "Computing the branches, singularity trace, and critical points of single degree-of-freedom, closed-loop linkages". Journal of Mechanisms and Robotics, **6**(7), p. 011006.

[2] Li, L., Myszka, D. H., Murray, A. P., and Wampler, C. W., 2013. "Using the singularity trace to understand linkage motion characteristics". In Proceedings of IDETC/CIE 2013, p. 13244.

[3] Norton, R. L., 1999. Design of Machinery: An Introduction to the Synthesis and Analysis of Mechanisms and Machines, 2 ed. McGraw-Hill, New York.

[4] Erdman, A. G., Sandor, G. N., and Kota, S., 2001. Mechanism Design: Analysis and Synthesis, 4 ed., Vol. 1. Prentice Hall, New Jersey.

[5] Kovacs, P., and Hommel, G., 1993. "On the tangent-half-angle substitution". In Computational Kinematics, J. Angeles, ed. Kluwer Academic Publishers, Norwell, MA, pp. 27–39.

[6] Porta, J. M., Ros, L., Creemers, T., and Thomas, F., 2007. "Box approximations of planar linkage configuration spaces". Journal of Mechanical Design, **129**(4), pp. 397–405.

[7] Wampler, C. W., 1999. "Solving the kinematics of planar mechanisms". Journal of Mechanical Design, **121**(3), pp. 387–391.

[8] Gregorio, R. D., 2007. "A novel geometric and analytic technique for the singularity analysis of one-dof planar mechanisms". Mechanism and Machine Theory, **42**, February, pp. 1462–1483.

[9] Gosselin, C., and Angeles, J., 1990. "Singularity analysis of closed-loop kinematic chains". IEEE Transactions on Robotics and Automation, **6**(3), pp. 281–290.

[10] Park, F., and Kim, J. W., 1999. "Singularity analysis of closed kinematic chains". Journal of mechanical design, **121**(1), pp. 32–38.

[11] Di Gregorio, R., 2009. "A novel method for the singularity analysis of planar mechanisms with more than one degree of freedom". Mechanism and Machine Theory, **44**(1), pp. 83–102.

[12] Zlatanov, D., Fenton, R. G., and Benhabib, B., 1994. "Singularity analysis of mechanisms and robots via a motion-space model of the instantaneous kinematics". In Robotics and Automation, 1994. Proceedings., 1994 IEEE International Conference on, IEEE, pp. 980–985.

[13] Balli, S. S., and Chand, S., 2002. "Defects in link mechanisms and solution rectification". Mechanism and Machine Theory, **37**(9), pp. 851–876.

[14] Yan, H.-S., and Wu, L.-l., 1989. "On the dead-center positions of planar linkage mechanisms". Journal of Mechanical Design, **111**(1), pp. 40–46.

[15] Chase, T. R., and Mirth, J. A., 1993. "Circuits and branches of single-degree-of-freedom planar linkages". Journal of Mechanical Design, **115**(2), pp. 223–230.

[16] Murray, A. P., Turner, M. L., and Martin, D. T., 2008. "Synthesizing single dof linkages via transition linkage identification". Journal of Mechanical Design, **130**, February, p. 022301.

[17] Larochelle, P., and Venkataramanujam, V., 2013. "A new concept for reconfigurable planar motion generators". In Proceedings of IMECE2013, p. 62571.

[18] Larochelle, P., and Venkataramanujam, V., 2014. "Analysis of planar reconfigurable motion generators". In Proceedings of IDETC/CIE 2014, p. 34242.

[19] Tao, D. C., 1964. Applied Linkage Synthesis. Addison-Wesley,Reading, MA.

[20] Chuenchom, T., and Kota, S., 2007. "Synthesis of programmable mechanisms using adjustable dyads". Journal of Mechanical Design, **119**(2), pp. 232–237.

[21] Bates, D. J., Hauenstein, J. D., Sommese, A. J., and Wampler II, C. W., 2008. "Software for numerical algebraic geometry: a paradigm and progress towards its implementation". In Software for algebraic geometry. Springer, pp. 1–14.

[22] Merlet, J.-P., 2004. "Solving the forward kinematics of a gough-type parallel manipulator with interval analysis". The International Journal of robotics research, **23**(3), pp. 221–235.

[23] Mourrain, B., and Pavone, J. P., 2009. "Subdivision methods for solving polynomial equations". Journal of Symbolic Computation, **44**(3), pp. 292–306.

[24] Merlet, J.-P., 2007. "A formal-numerical approach for robust in-workspace singularity detection". Robotics, IEEE Transactions on, **23**(3), pp. 393–402.

[25] Kotlarski, J., De Nijs, R., Abdellatif, H., and Heimann, B., 2009. "New interval-based approach to determine the guaranteed singularity-free workspace of parallel robots". In Robotics and Automation, 2009. ICRA'09. IEEE International Conference on, IEEE, pp. 1256–1261.

[26] Mourrain, B., Pavone, J.-P., and Trébu, P. "et, elias p. tsigaridas, and julien wintz. synaps, a library for dedicated applications in symbolic numeric computations". IMA Volumes in Mathematics and its Applications, pp. 81–110.

[27] Bates, D. J., Hauenstein, J. D., Sommese, A. J., and Wampler, C. W., 2013. Numerically Solving Polynomial Systems with Bertini. Society for Industrial and Applied Mathematics, Philadelphia.

[28] Bates, D. J., Hauenstein, J. D., Sommese, A. J., and Wampler, C. W. Bertini: Software for numerical algebraic geometry. Available at bertini.nd.edu with permanent doi: dx.doi.org/10.7274/R0H41PB5.

[29] Galletti, C. U., 1986. "A note on modular approaches to planar linkage kinematic analysis". Mechanism and Machine Theory, **21**(52), pp. 385–391.

[30] Persinger, J. A., Schmiedeler, J. P., and Murray, A. P., 2009. "Synthesis of planar rigid-body mechanisms approximating shape changes defined by closed curves". Journal of Mechanical Design, **131**(7), p. 071006.

[31] Zhao, K., Schmiedeler, J. P., and Murray, A. P., 2012. "Design of planar, shape-changing rigid-body mechanisms for morphing aircraft wings". Journal of Mechanisms and Robotics, **4**(4), p. 041007.

[32] Giaier, K., Myszka, D. H., Kramer, W. P., and Murray, A. P., 2014. “Variable geometry dies for polymer extrusion”. In Proceedings of IMECE2014, p. 38409.